The Astrophysical Journal, 833:206 (6pp), 2016 December 20 doi:10.3847/1538-4357/833/2/206

VERY LONG-PERIOD PULSATIONS BEFORE THE ONSET OF SOLAR FLARES

Baolin Tan[1,2], Zhiqiang Yu[2,3], Jing Huang[1,2], Chengming Tan[1,2], and Yin Zhang[1]
[1] Key Laboratory of Solar Activity, National Astronomical Observatories of Chinese Academy of Sciences, Beijing 100012, China; bltan@nao.cas.cn
[2] School of Astronomy and Space Sciences, University of Chinese Academy of Sciences, Beijing 100049, China
[3] Applied Physics Department, Harbin Institute of Technology, Harbin, Heilongjiang 15001, China
Received 2016 September 16; revised 2016 October 26; accepted 2016 October 26; published 2016 December 19

ABSTRACT

Solar flares are the most powerful explosions occurring in the solar system, which may lead to disastrous space weather events and impact various aspects of our Earth. It remains a big challenge in modern astrophysics to understand the origin of solar flares and predict their onset. Based on the analysis of soft X-ray emission observed by the *Geostationary Operational Environmental Satellite*, this work reports a new discovery of very long-periodic pulsations occurring in the preflare phase before the onset of solar flares (preflare-VLPs). These pulsations typically have periods of 8–30 min and last for about 1–2 hr. They are possibly generated from LRC oscillations of plasma loops where electric current dominates the physical process during magnetic energy accumulation in the source region. Preflare-VLPs provide essential information for understanding the triggering mechanism and origin of solar flares, and may be a convenient precursory indicator to help us respond to solar explosions and the corresponding disastrous space weather events.

Key words: plasmas – stars: coronae – Sun: atmosphere – Sun: corona

1. INTRODUCTION

A solar flare is a sudden, rapid, and violent magnetic-energy release and brightness enhancement in a broad spectrum of emissions observed in the solar atmosphere near sunspots (Shibata & Magara 2011). Generally, solar flares are classified as A-, B-, C-, M-, and X-class according to their maximum flux at soft X-ray (SXR) wavelengths of 1.0–8.0 Å as measured by the standard *Geostationary Operational Environmental Satellite* (*GOES*, a satellite series initially deployed in 1974; *GOES-14* and *GOES-15* are inline during the present solar cycle 24) (Tandberg-Hanssen & Emslie 1988). A typical X-class flare may release magnetic energy of more than 10^{25} J into interplanetary space and impact greatly upon various aspects of our Earth (Nonweiler 1958; Scafetta & West 2003; Pick & Vilmer 2008; Gonzalez et al. 2014). Although there is a general agreement on the flares' causes of magnetic reconnection in the solar atmosphere, there are still many unresolved problems: what is the trigger of magnetic reconnection in the source region? How does the enormous magnetic energy transform into kinetic energy carried by particles and plasma? In particular, how do we predict a powerful solar flare and any related disastrous space weather event? Naturally, it is very important and relatively easy to determine the precursors of solar flares. So far, many clues have been reported from multi-wavelength observations in preflare phases, including radio spectral fine structures (Zhang et al. 2015), filament activities (Chifor et al. 2006), weak SXR bursts (Tappin 1991), magnetic helicity accumulations (Zhang et al. 2008), etc. However, some of these are very weak, with considerable uncertainties, and some of them are very complicated and difficult to recognize from the vast ocean of observational data (Martin 1980; Bloomfield et al. 2012).

Generally, a solar flare can be partitioned into three phases according to its *GOES* SXR flux light curve at wavelength of 1.0–8.0 Å: preflare (before the flare onset), rising (from the flare onset to its maximum; the time interval is known as the rising-time of the flare) and postflare (after the flare maximum). A typical flare event and its phase partition are shown in Figure 1.

Because the *GOES* program consists of a series of geostationary satellites which overlap in time, there are always one to three spacecraft working in orbit, and this guarantees an essentially uninterrupted time series of recorded solar SXR fluxes (Thomas et al. 1985; Garcia 1994; White et al. 2005). In this work, we mainly investigated the *GOES* SXR observation data during the preflare phase, and found that there were very long-period pulsations (VLPs) with typical periods of 8–30 min and typical duration of about 1–2 hr occurring just before the onset of solar flares. We name these phenomena preflare-VLPs. As we know, VLPs with similar timescales are frequently reported during flare processes or even a non-flaring Sun (Harrison 1987; Svestka 1994; Tan et al. 2010; Wang 2011; Yuan et al. 2011, etc.). However, the preflare-VLPs reported in this work are, for the first time, observed just in the preflare phase, and may be meaningful in addressing the questions mentioned above.

This paper is organized as follows. Section 2 introduces the main properties of preflare-VLPs in several typical flare events and Section 3 presents the statistical characteristics of solar flares in solar cycle 24. The physical mechanism and related theoretical discussions are presented in Section 4, and conclusions are summarized in Section 5.

2. TYPICAL FLARE EVENTS ACCOMPANYING PREFLARE-VLPS

In order to eliminate the influence of other flares, this work focuses on analyzing isolated flares in solar cycle 24 observed by *GOES* at SXR wavelengths of 1.0–8.0 Å and 0.5–4.0 Å with a cadence of 2 s, which in principle probes the dynamical process of energy release in flaring active regions (Tandberg-Hanssen & Emslie 1988; Georgoulis et al. 2001). Here, an isolated solar flare is defined as having no similar or higher class flare event occurring 2 hr before the flare onset, and no saturation or bad recorded data to disturb the analysis results.

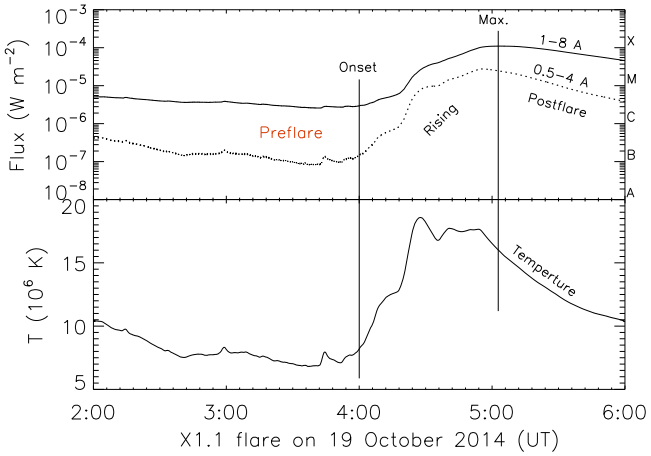

Figure 1. Flare classification and the phase partition. The top panel is the soft X-ray light curves at 1–8 Å and 0.5–4 Å, while the bottom presents the profile of the corresponding temperature.

Figure 2 presents SXR light curves at 1.0–8.0 Å and 0.5–4.0 Å, and the related temperatures in four typical flare events. The temperature is derived from the ratio of SXR intensities at the above two wavelength bands (Thomas et al. 1985; White et al. 2005). All background emission is subtracted from the SXR flux intensity. By casual inspection, we find that there are trains of pulses with approximately equal time intervals occurring before the onset of the corresponding flare event. We call this train of pulses a preflare-VLP. Here, it is necessary to define the detection criteria of preflare-VLPs: (1) they occur at most 2 hr before the flare onset, (2) they last more than 30 minutes (duration $D > 30$ min) and are composed of at least four pulses, (3) the maximum amplitude of each pulse is higher than 2σ (σ is the standard derivation of the background temperature before the train of pulses), and (4) the time interval between adjacent pulses is called the period (P), and the maximum period is shorter than twice the minimum period ($P_{\max} < 2P_{\min}$), and $P > 1$ min. When there is a pulsation satisfying the above criteria 2 hr before the flare onset, we say the flare is accompanied by a preflare-VLP, and when there is no such pulsation we say the flare is without a preflare-VLP.

2.1. X2.0 Flare on 2014 October 26

Figure 2(A) shows the process of an X2.0 flare occurring on 2014 October 26. The flare took place in a super active region NOAA12192, located at S14W37, close to the center of the solar disk. The flare started at 10:35 UT, reached a maximum at 10:56 UT, and the rising-time was about 21 min. During the two hour preflare phase before the onset, from 08:30 UT to 10:35 UT, there was no flare stronger than M-class. Therefore the X2.0 flare is an isolated flare event.

During the preflare phase of the X2.0 flare, there is a preflare-VLP which contains seven pulses and lasts for about 80 min. The pulse period is in the range of 9.5–13.0 min, and the average period is about 11.4 min (684 s). It is very interesting that the pulse amplitudes increase slowly from about 1.0 to 4.0 MK of the temperature profile. The preflare-VLP can be fitted by a cosine function from a least-squares method,

$$T \approx 5.0 + 10^{-3}t + 6.1 \times 10^{-8}t^2 \cos\left(\frac{2\pi t}{684}\right) \quad (1)$$

where T is the temperature in units of 10^6 K (MK), and $t$is time in seconds and starts from 08:30 UT. The constant 5.0 MK is the average temperature of the background before the preflare-VLP. The second term $10^{-3}t$ represents the slow changes of the background during the preflare-VLP. The function $6.1 \times 10^{-8}t^2$ in the third term shows the change of the amplitude of the pulsation. Here, the period of the pulsation is nearly constant (684 s).

2.2. X2.7 Flare on 2015 May 05

Figure 2(B) shows an X2.7 flare occurring on 2015 May 05 in active region NOAA12339, located at N15E79, very close to the east limb of the solar disk. The flare started at 22:05 UT, rapidly reached its maximum at 22:10 UT, and the rising-time was only 5 min. During the preflare phase from 20:00 UT to 22:05 UT, there was also no flare stronger than M-class. Therefore this flare is an isolated flare event.

During the preflare phase, there is a preflare-VLP which contains four pulses and lasts for about 70 min. The pulse period is in range of 16.0–20.0 min, and the average period is about 18.4 min (1104 s). Similarly, the pulse amplitudes increase from about 0.5 to 5.5 MK of the temperature profile. We can also apply a cosine function from a least-squares method to fit the preflare-VLP,

$$T \approx 3.5 + 8.0 \times 10^{-4}t + 1.2 \times 10^{-7}t^2 \cos\left(\frac{2\pi t}{1104}\right). \quad (2)$$

Here, t starts from 20:00 UT. This fitted function is very similar to Equation (1); the average temperature of the background before the preflare-VLP is only about 3.5 MK.

2.3. M2.9 Flare on 2013 October 25

Figure 2(C) shows an M2.9 flare occurring on 2013 October 25 in active region NOAA11882, at S07E76, close to the east limb of the solar disk. The flare started at 02:48 UT, peaked at 03:02 UT, and the rising-time was about 14 min. It is also an isolated flare.

Before the flare onset, there is a preflare-VLP containing seven pulses and lasting for about 130 min. The pulse period increases from 15 min to 30 min, and the average period is about 21.2 min. The pulse amplitude increases in the first half and then decreases slowly in the second half of the preflare-VLP, which can be also fitted by a complex cosine function,

$$T \approx 7.0 - 5 \times 10^{-5}t + \left(\frac{5000}{t - 4800}\right)^2 \cos\left[\frac{(18200 - t)\pi}{2.88 \times 10^6}(t + 200)\right]. \quad (3)$$

t starts from 23:30 UT on 2013 October 24. Here, the average temperature of the background before the preflare-VLP is 7.0 MK, and the change of the background temperature during the preflare-VLP is negative, contrary to Equations (1) and (2) At the same time, the period and amplitude of the pulsation show more complicated changes with time.

2.4. C2.4 Flare on 2012 July 13

Figure 2(D) shows a small C2.4 flare occurring on 2012 July 13 in active region NOAA11515, at S19E10, near the center of the solar disk. The flare started at 06:22 UT, reached its

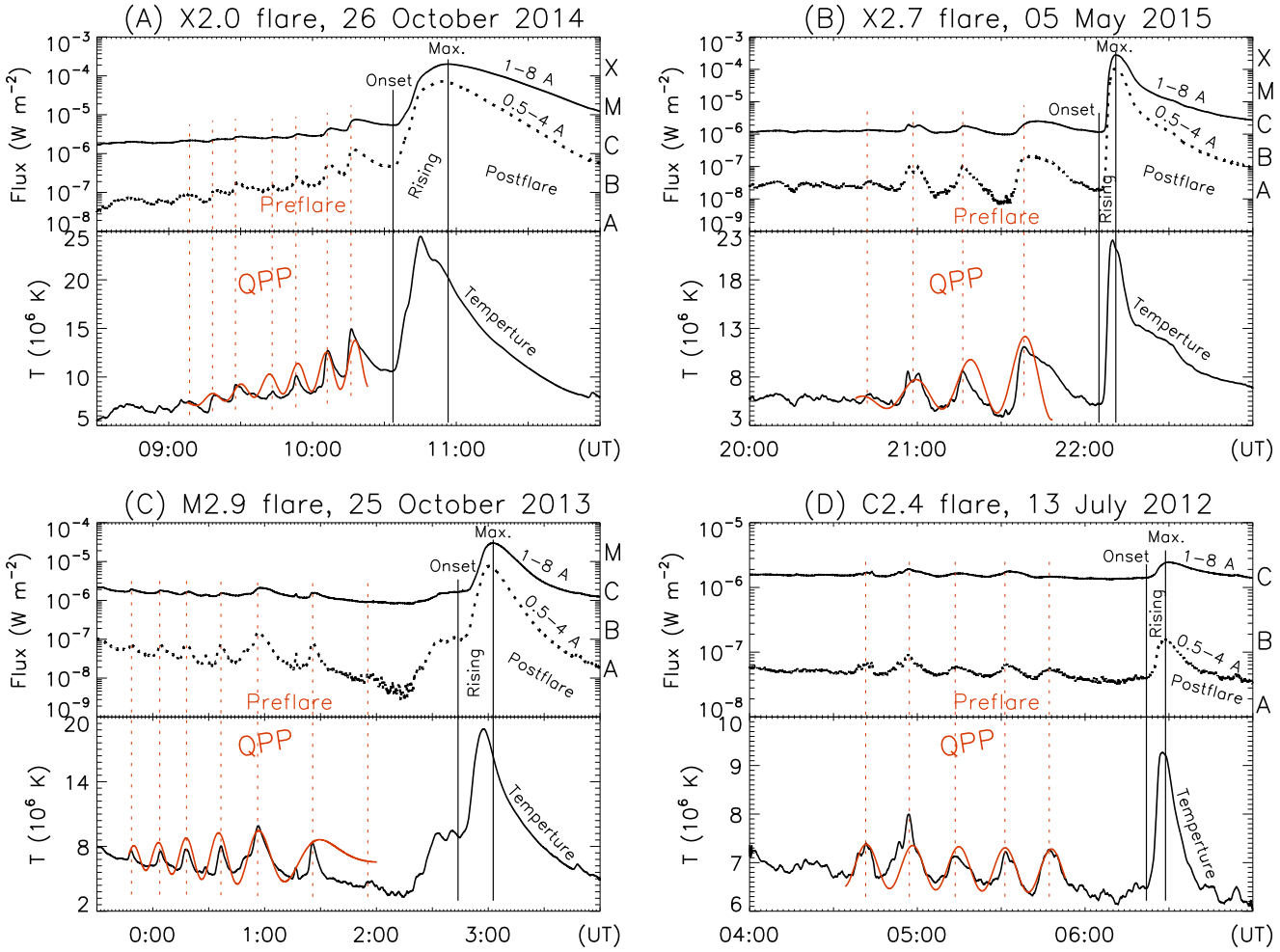

Figure 2. Very long-period pulsations before the onset of solar flares (preflare-VLPs) in four typical solar flares. In each event, the top panel shows light curves of soft X-ray emission flux at wavelengths of 1.0–8.0 Å and 0.5–4.0 Å, while the bottom panel shows a profile of the corresponding temperature. The observations are from *GOES-15*. The vertical dotted lines mark pulses of the preflare-VLP.

maximum at 06:29 UT, and the rising-time was about 7 min. It is still an isolated flare event.

During the preflare phase, a preflare-VLP occurs with five pulses and lasts for about 75 min. The pulse period is in the range of 15.0–17.0 min with an average of 16.4 min (984 s). We can also use a cosine function to fit the preflare-VLP,

$$T \approx 7.0 - 2.5 \times 10^{-5} t + 0.45 \cos\left(\frac{2\pi t}{984} + 1.5\right). \quad (4)$$

t starts from 04:00 UT on 2012 July 13. Similar to Equation (3), here the average temperature of the background before the preflare-VLP is about 7.0 MK, and the change of the background temperature during the preflare-VLP is negative. Both the amplitude and period are nearly constant.

Furthermore, Figure 2 also shows that the preflare-VLP at 1.0–8.0 Å is fully in phase with that at 0.5–4.0 Å as well as at the corresponding temperature profiles. The amplitude of temperature variation is in the range 0.5–5.5 MK. This indicates that the temperature of the flaring region also experiences quasi-periodic variations before the flare onset.

In the above descriptions, we have just presented the results derived directly from counting the pulses of the preflare-VLP, displayed very simply and straightforwardly. To check the results, we also applied two mathematical analytic methods, fast Fourier transformation (FFT) and wavelet transformation (WLT), to the time-series temperature data, and found the results to be in agreement with each other.

3. STATISTICAL ANALYSIS OF THE PREFLARE-VLP IN SOLAR CYCLE 24

In order to demonstrate the universality of the preflare-VLP, we carried out a statistical investigation of isolated solar flares. Using the detection criteria described in Section 2, we distinguished a total of 412 isolated flares in solar cycle 24 (from 2010 October to 2016 July), including 39 X-class, 183 M-class, and 190 C-class flares. We applied three different methods to distinguish the emission periodicity in the preflare phase of the above flare events: (1) directly counting the pulses, (2) FFT, and (3) WLT, and authenticated each securely.

Among the 412 isolated flares, there are 144 (~35%) with preflare-VLPs, including 18 X-class (46%), 76 M-class (42%), and 50 C-class (26%) flares. The other 268 flares have no obvious preflare-VLP. Table 1 presents the statistical results of the period and duration of the preflare-VLPs, and the rising-time of the isolated flares. Figure 3 presents their distributions with respect to flare class.

From Table 1 and Figure 3, we can obtain several interesting conclusions.

Table 1
Preflare-VLP Statistics of the Isolated Flares in Solar Cycle 24

Type	Parameter	X-class	M-class	C-class
with preflare-VLP	Number	18(46%)	76(42%)	50(26%)
	Period (minute)	4.4–47.3 (16.1 ± 10.7)	1.9–46.2 (16.2 ± 7.9)	7.7–33.3 (16.4 ± 7.4)
	Duration (minute)	45–180 (85.6 ± 33.7)	17–200 (98.5 ± 35.8)	42–185 (97.4 ± 33.2)
	Rising-time (minute)	4–33 (14.7 ± 9.1)	2–47 (11.7 ± 9.5)	3–36 (9.8 ± 8.3)
without preflare-VLP	Number	21(54%)	107(58%)	140 (74%)
	Rising-time (minute)	6–95 (25.2 ± 23.0)	2–103 (16.7 ± 16.5)	3–78 (13.2 ± 11.8)

Note. The format of the numerical value of period, duration, and rising-time is: minimum–maximum (average ± mean square deviation). The percentage in the parentheses is the proportion in the same flare class.

(1) Each preflare-VLP lasts for about 30–200 min (the typical duration is in the range 60–120 min, i.e., 1–2 hr) and contains 4–11 pulses. The typical pulsating period is in the range 8–30 min. The longest period is 47 min (X1.0 flare, 11 June 2014) and the shortest is 1.9 min (M1.0 flare, 2013 November 5). The averages are 16.4 ± 7.4, 16.2 ± 7.9, and 16.1 ± 10.7 min in the C-, M-, and X-class flares, respectively, just around a typical value of 16 ± 8 min. Here, the values following the symbol ± are statistical mean square deviations.

(2) There is almost no obvious correlation between the timescales (P and D) of preflare-VLPs and the *GOES* SXR classes of the host flares. The difference in the average periods is very small between different flare classes.

(3) The stronger flares have higher probability to produce preflare-VLPs as well as flares with shorter rising-times. For example, there are about 46% X-class flares have preflare-VLPs as opposed to only 26% in C-class flares. The average rising-times of C-, M-, and X-class flares with preflare-VLPs are 9.8 ± 8.3, 11.7 ± 9.5, and 14.7 ± 9.1 min, while the values for those without preflare-VLPs are 13.2 ± 11.8, 16.7 ± 16.5, and 25.2 ± 23.0 min, respectively. The longest rising-time of a flare with a preflare-VLP is shorter than 48 min, while all flares with rising-times above 50 min have no preflare-VLPs.

Figure 1 presents a typical example of a long-rising X-class flare without a preflare-VLP. The rising-time is 63 min. There is no obvious pulse during the 2 hr preflare phase. Long-rising flares may release energy relatively slowly in complex multi-loop system, and the plasma loops may disturb each other, which drives the dynamic processes to become very complicated, obscuring the signal of preflare-VLPs from the observations.

In Section 2, we applied some cosine functions from the least-squares method to fit the preflare-VLP in Equations (1)–(4). We can summarize the fitted function in a unified format:

$$T = T_0 + bt + M(t)\cos\left(\frac{2\pi}{P}t\right). \quad (5)$$

Here, T_0 is the average temperature of the background active region before the preflare-VLP.

b is the growth rate of the average temperature of the background during the preflare-VLP. It is positive ($b > 0$) in most flare events, such as the X2.0 flare on 2014 October 26 and the X2.7 flare on 2015 May 5. However, it is remarkable that b is negative in some events, such as the M2.9 flare on 2013 October 25 and the C2.4 flare on 2013 July 13 ($b < 0$). Statistics indicate that there are about 20% flare events with decreasing mean temperature during the preflare phase $b < 0$.

$M(t)$ is the pulse amplitude of the preflare-VLP which is generally a function of time. In the X2.0 flare on 2014 October 26, $M(t) = 6.1 \times 10^{-8}t^2$ which is increasing with time. In the M2.9 flare on 2013 May 25 $M(t) = \left(\frac{5000}{t-4800}\right)^2$. But in the case of the C2.4 flare on 2012 July 13, $M(t) = 0.45$ is approximately constant.

P is the period of the preflare-VLP which is generally a constant in most events, for example, $P = 684$ s in the X2.0 flare on 2014 October 26, $P = 1104$ s in the X2.7 flare on 2015 May 5, and $P = 984$ s in the C2.4 flare on 2012 July 13. However, in the case of the M2.9 flare on 2013 October 25, $P = \frac{5.78 \times 10^6}{18200 - t}$ is increasing with time.

4. GENERATION MECHANISM OF PREFLARE-VLPS

What is the cause of the formation of VLPs during the preflare phase?

As we know, quasi-periodic pulsations (QPPs) with periods from subseconds to several minutes in multi-wavelength observations occur during the flare rising and postflare phases (Aschwanden 1987; Kupriyanova et al. 2010; Tan et al. 2010; Simoes et al. 2015, etc.). Magnetohydrodynamic (MHD) oscillations are generally applied to explain the formation of QPPs, because MHD oscillations can affect almost all aspects of the emission process: magnetic reconnection and rate modulation, electron acceleration and dynamics, and plasma conditions. Periods and other parameters are linked with properties of emitting plasmas and the morphology of magnetic fields (Roberts et al. 1984; Aschwanden 1987; Nakariakov & Melnikov 2009). Foullon et al. (2005) reported long-period pulsations with timescales of 8–12 min of X-ray radiation during solar flares and interpreted them as a periodic pumping of electrons in a compact flaring loop modulated by MHD oscillation. Others have suggested that such pulsations might be related to the slow-mode oscillations in large scale coronal loops (Svestka 1994), while it has also been suggested that the long-period pulsations could be associated with gravity-driven solar interior modes and connected with the wave leakage of chromospheric oscillations (Yuan et al. 2011). Another possible explanation for VLPs is the thermal overstability of standing slow magnetoacoustic waves in the magnetic flux loops (Kumar et al. 2016), such as the SUMER oscillations with periods in the range 5–40 min and detected in long loops with lengths of 200–300 Mm (Wang 2011).

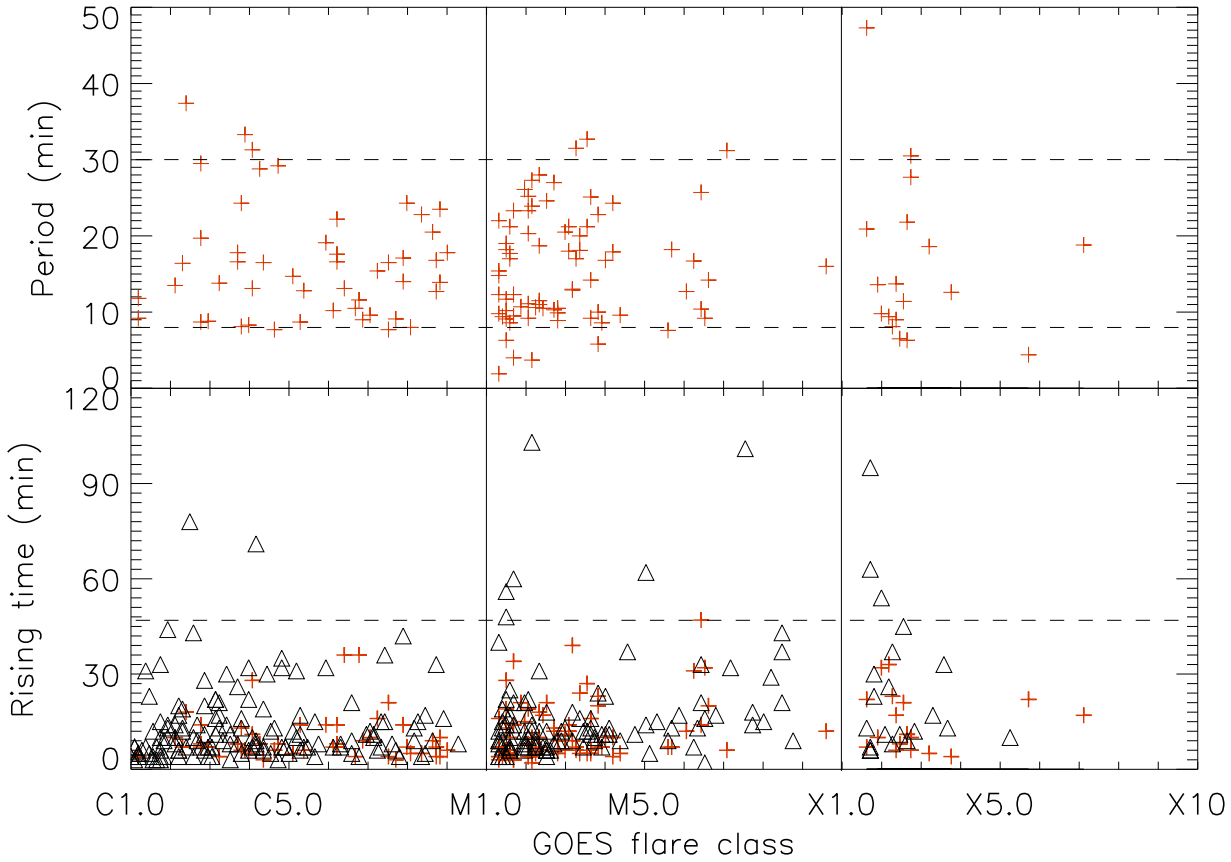

Figure 3. Statistics of the isolated C- (left), M- (middle) and X-class flares (right) in solar cycle 24. The top panels are period distributions of the preflare-VLPs, and the bottom panels show the rising-time distribution of the isolated flares. Red plus symbols (+) indicate flares with preflare-VLPs while triangles (△) indicate flares without preflare-VLPs.

The MHD oscillation mode should be the most favorable candidate for explaining the formation of VLPs. However, when we utilize this mechanism to demonstrate the formation of preflare-VLPs, we encounter some serious questions: the flare explosion may be the trigger of VLPs during the flare, but what is the trigger of the oscillations before the flare onset without explosions? And how do we make a natural connection with the details of energy accumulation in the preflare phase?

Actually, the preflare-VLP is much like the quasi-periodic oscillations in the precursor phase of a tokamak major disruption (Wesson 1997; Jiang et al. 2015). The precursor phase (similar to the preflare phase) lasts for typically 10 ms and the fast phase (similar to the flare rising phase) lasts for about 1 ms in medium-sized tokamaks. Because of electric currents and limited resistivity, the tearing-mode instability can give rise to the growth of magnetic oscillations of an $m = 2$ mode in the precursor phase of a tokamak major disruption (Jiang et al. 2015).

Similar to tokamaks, solar flaring loops also have longitudinal electric currents (Tan & Huang 2006; Tan et al. 2006). During the preflare phase, the flaring source region accumulates magnetic energy gradually through photospheric convection. This can drive shearing, rotating, and twisting motions around loop footpoints and drive electric currents in the plasma loop (Alfvén & Carlqvist 1967; Tobias & Cattaneo 2013). The current-carrying plasma loop is analogous to an LRC-circuit with electric inductance $L = \frac{\mu_0 l}{\pi}\left(\ln\frac{8l}{\sqrt{\pi S}} - \frac{7}{4}\right)$ and capacitance $C = \frac{8\pi\rho S^2}{\mu_0^2 I^2}$. Here, $\rho = n_e m_e + n_i m_i \approx n m_i$ is the plasma density in units of kg·m^{-3}, n is the plasma number density, S, l and I are the cross-sectional area (m^2), length of the plasma loop (m) and and electric current (A), respectively. Such an LRC-circuit will produce intrinsic oscillation (Zaitsev et al. 1998) with period

$$P = 2\pi\sqrt{LC} \approx 2.75 \times 10^4 \frac{S\sqrt{\rho}}{I}. \quad (6)$$

LRC oscillation can modulate both thermal and nonthermal emission. Thermal emission contributes to SXR emission while nonthermal emission contributes to hard X-ray emission and energetic particles. The period of LRC oscillation is proportional to the cross-sectional area (S), and counter-proportional to the electric current (I) in the loop. Typical values in the flaring coronal loop are: $n = 10^{16}$ m^{-3}, $l = 5 \times 10^7$ m, and the cross-sectional radius is $r = 5 \times 10^6$ m (Bray et al. 1991). Considering the period of preflare-VLPs is 1.9–47 min, the electric current will be about $I = 3.1 \times 10^9 - 7.6 \times 10^{10}$ A.

Are these estimated electric currents reasonable? Many authors have obtained a maximum current of 10^{12} A in an active region during a solar flare derived from vector magnetograph observations (Canfield et al. 1993; Tan et al. 2006, etc.). Recalling that an active region is always composed of several decades or hundreds of plasma loops, it is reasonable to suppose that the electric current will have a magnitude of 10^{10} A or lower in a single flaring plasma loop, especially in the preflare phase.

Spangler (2007) developed a new method to observe the radio signal from a remote quasar 3C228 when the emission

passes by the solar limb coronal loops, and obtained an electric current of 10^8–10^9 A in the coronal loops. In fact, during the flare rising phase, QPPs also occur frequently with periods from several seconds up to about 2 min (Simoes et al. 2015), which are shorter than the period of the above preflare-VLPs. If we apply the same LRC oscillation mechanism to explain them, a stronger electric current of 10^{10}–10^{12} A can be obtained. This is natural because the flaring plasma loop may become more unstable and generate stronger electric currents during the flare rising phase.

Long-rising flares tend not to have preflare-VLPs. It is possible that a long-rising flare may have a relatively slow energy release and the flaring loops may disturb each other. These mutual interferences cause the dynamic processes to become complex and obscure the evidence of preflare-VLPs from the observations.

5. SUMMARY

Based on an analysis of standard *GOES* SXR recorded data, we discovered and confirmed that at least one-third of solar flares are accompanied by preflare-VLPs, whose periods are typically in the range 8–30 min and which last for 1–2 hr. It is possible that these kinds of pulsations are associated with some MHD oscillation modes, similar to other QPPs occurring in the flare rising and postflare phases. At the same time, LRC oscillation is also a favorable mechanism to interpret the formation of a preflare-VLP, which is associated with current-carrying plasma loops. With LRC oscillation, the preflare-VLP may provide two important sources of information for understanding solar explosions.

(1) The existence of preflare-VLPs indicates that electric currents are generated in flaring plasma loops before the onset of flares. The current-carrying loop may drive plasma instabilities, modulate SXR emission, and produce preflare-VLPs. By studying the details of preflare-VLPs, we may reveal the real triggering mechanism of solar flares, the energy release, and development of the source regions.
(2) The preflare-VLP can be regarded as the precursor of a solar flare. It is very simple to distinguish and extract the signal of a preflare-VLP from the *GOES* SXR observation data. Also, the duration of 1–2 hr is long enough for us to respond to the influence of a powerful solar eruption. Therefore, preflare-VLPs can be regarded as convenient precursory indicators for predicting solar flares, along with the possibility of disastrous space weather events, and providing an early warning.

Actually, besides the *GOES* SXR observation data, it is possible that we can obtain much more information on the preflare-VLP from next-generation, long-term continuous observations. For example, the imaging observation of the Atmospheric Imaging Assembly onboard NASA's satellite *Solar Dynamic Observatory* (*SDO*/AIA, Lemen et al. 2012) may provide abundant imaging information about thermal emission in the source regions with high spatial resolution. Additionally, the Chinese Spectral Radioheliograph (CSRH, Yan et al. 2009, now renamed the Mingantu Spectral Radioheliograph, MUSER) can provide not only nonthermal broadband spectral structures, but also variations of location and shape in the source region with very high resolution.

The authors thank the referee for helpful and valuable comments on this paper. We also thank the *GOES* teams for providing perfect observation data and excellent software for data analysis. This work is supported by NSFC grant 11273030, 11661161015, 11221063, 11373039, 11573039, and 2014FY120300, CAS XDB09000000.

REFERENCES

Alfvén, H., & Carlqvist, P. 1967, SoPh, 1, 220
Aschwanden, M. J. 1987, SoPh, 111, 113
Bloomfield, D. S., Higgins, P. A., McAteer, R. T. J., & Gallagher, P. T. 2012, ApJL, 747, L41
Bray, R. J., Cram, L. E., Durrant, C. J., & Loughhead, R. E. 1991, Plasma Loops in the Solar Corona (Cambridge: Cambridge Univ. Press)
Canfield, R. C., de La Beaujardiere, J.-F., Fan, Y. H., et al. 1993, ApJ, 411, 362
Chifor, C., Mason, H. E., Tripathi, D., Isobe, H., & Asai, A. 2006, A&A, 458, 965
Foullon, C., Verwichte, E., Nakariakov, V. M., & Fletcher, L. 2005, A&A, 440, L59
Garcia, H. A. 1994, SoPh, 154, 275
Georgoulis, M. K., Vilmer, N., & Crosby, N. B. 2001, A&A, 367, 326
Gonzalez, H. I., Komm, R., Pevtsov, A., & Leibacher, J. W. 2014, SoPh, 289, 437
Harrison, R. A. 1987, A&A, 182, 337
Jiang, M., Hu, D., Wang, X. G., et al. 2015, NucFu, 55, 083002
Kumar, S., Nakariakov, V. M., & Moon, Y.-J. 2016, ApJ, 824, 8
Kupriyanova, E. G., Melnikov, V. F., Nakariakov, V. M., & Shibasaki, K. 2010, SoPh, 267, 329
Lemen, J. R., Title, A. M., Akin, D. J., et al. 2012, SoPh, 275, 17
Martin, S. 1980, SoPh, 68, 217
Nakariakov, V. M., & Melnikov, V. F. 2009, SSRv, 149, 119
Nonweiler, T. 1958, Natur, 182, 468
Pick, M., & Vilmer, N. 2008, A&ARv, 16, 1
Roberts, B., Edwin, P. M., & Benz, A. O. 1984, ApJ, 279, 857
Scafetta, N., & West, B. J. 2003, PhRvL, 90, 248701
Shibata, K., & Magara, T. 2011, LRSP, 8, 6
Simoes, P. J. A., Hudson, H. S., & Fletcher, L. 2015, SoPh, 290, 3625
Spangler, S. R. 2007, ApJ, 670, 841
Svestka, Z. 1994, SoPh, 152, 505
Tan, B. L., & Huang, G. L. 2006, A&A, 453, 321
Tan, B. L., Ji, H. S., Huang, G. L., et al. 2006, SoPh, 239, 137
Tan, B. L., Zhang, Y., Tan, C. M., & Liu, Y. Y. 2010, ApJ, 723, 25
Tandberg-Hanssen, E., & Emslie, A. 1988, The Physics of Solar Flares (Cambridge: Cambridge Univ. Press)
Tappin, S. J. 1991, A&AS, 87, 277
Thomas, R. J., Starr, R., & Crannell, C. J. 1985, SoPh, 95, 323
Tobias, S. M., & Cattaneo, F. 2013, Natur, 497, 461
Wang, T. J. 2011, SSRv, 158, 397
Wesson, J. 1997, Tokamak (Oxford: Clarendon)
White, S. M., Thomas, R. J., & Schwarts, R. A. 2005, SoPh, 227, 231
Yan, Y. H., Zhang, J., Wang, W., et al. 2009, EM&P, 104, 97
Yuan, D., Nakariakov, V. M., Chorley, N., & Foullon, C. 2011, A&A, 533, 116
Zaitsev, V. V., Stepanov, A. V., Urpo, S., & Pohjolainen, S. 1998, A&A, 337, 887
Zhang, Y., Tan, B. L., Karlicky, M., et al. 2015, ApJ, 799, 30
Zhang, Y., Tan, B. L., & Yan, Y. H. 2008, ApJL, 682, L133